Springer Theses

Photomodulated Optical Reflectance

A Fundamental Study Aimed at Non-Destructive Carrier Profiling in Silicon

Bearbeitet von
Janusz Bogdanowicz

1. Auflage 2012. Buch. xxiv, 204 S. Hardcover
ISBN 978 3 642 30107 0
Format (B x L): 15,5 x 23,5 cm
Gewicht: 508 g

Chapter 2
Theory of Perturbation of the Reflectance

In this chapter, we assume a small perturbation of the complex refractive index $\tilde{n}(x, y, z, t)$ is somehow generated (e.g. by doping, optically injected carriers and/or heat,...) in a homogeneous silicon sample and we calculate how this perturbation impacts the reflectance $R(x, y, t)$ of a probe laser shining on the sample.

In all generality, the perturbed refractive index reads

$$\tilde{n}(x, y, z, t) = \tilde{n}_0 + \Delta\tilde{n}_0(x, y, z) + \underbrace{\Delta\tilde{n}_1(x, y, z)\cos[\omega t - \phi_1(x, y, z)]}_{\text{fundamental}} + \sum_{j=2}^{+\infty} \underbrace{\Delta\tilde{n}_j(x, y, z)\cos[j\omega t - \phi_j(x, y, z)]}_{j\text{th harmonic}}, \tag{2.1}$$

where $\tilde{n}_0$ is the refractive index of the unperturbed silicon sample, $\Delta\tilde{n}_0(x, y, z)$ is the time-independent component of the perturbation of the refractive index, $\Delta\tilde{n}_1(x, y, z)$ and $\phi_1(x, y, z)$ are respectively the amplitude and phase of the fundamental mode of the perturbation, $\Delta\tilde{n}_j(x, y, z)$ and $\phi_j(x, y, z)$ $(j = 2, 3, \ldots)$ are respectively the amplitude and phase of the jth harmonic of the perturbation. Note that $\tilde{n}_0$ and $\Delta\tilde{n}_j(x, y, z)$ $(j = 0, 1, \ldots)$ are all complex numbers. In this chapter and the following, ω can be understood in all generality as the fundamental angular frequency of the refractive index perturbation but, it will become clear in Chap. 4 that ω is the angular modulation frequency of the pump laser irradiance.

As a result of this perturbation, a probe laser shining on the sample is reflected with a perturbed reflectance $R(x, y, t)$ such that

$$R(x, y, t) = R_0 + \Delta R_0(x, y) + \underbrace{\Delta R_1(x, y)\cos[\omega t - \Phi_1(x, y)]}_{\text{fundamental}} + \sum_{j=2}^{+\infty} \underbrace{\Delta R_j(x, y)\cos[j\omega t - \Phi_j(x, y)]}_{j\text{th harmonic}}, \tag{2.2}$$

J. Bogdanowicz, *Photomodulated Optical Reflectance*, Springer Theses,
DOI: 10.1007/978-3-642-30108-7_2, © Springer-Verlag Berlin Heidelberg 2012

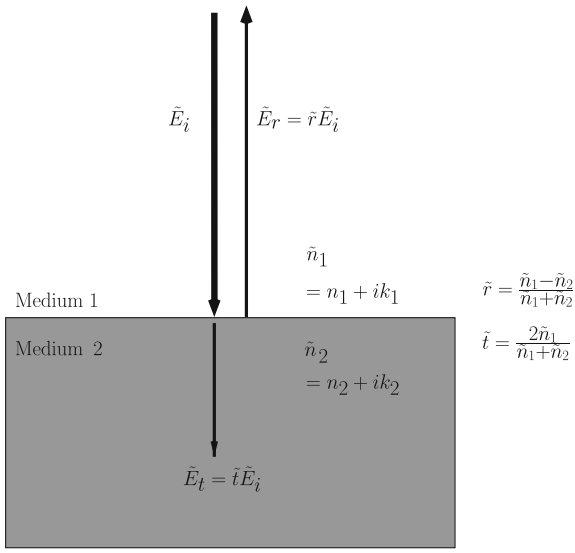

Fig. 2.1 An electromagnetic wave with electric field $\tilde{E}_i$ incident on an interface between two media of respective refractive indices $\tilde{n}_1$ and $\tilde{n}_2$ is partially reflected with electric field $\tilde{E}_r$ and transmitted with electric field $\tilde{E}_t$. The ratio between the reflected (resp. transmitted) and incident electric fields is given by $\tilde{r}$ (resp. $\tilde{t}$) which follows Fresnel's reflection formula (2.3) [resp. (2.4)]

where R_0 is the reflectance of the unperturbed Si sample, $\Delta R_0(x, y)$ is the time-independent component of the perturbation of the reflectance, $\Delta R_1(x, y)$ and $\Phi_1(x, y)$ are the magnitude and phase of its fundamental mode and $\Delta R_j(x, y)$ and $\Phi_j(x, y)$ $(j = 2, 3, \ldots)$ are the magnitude and phase of its jth harmonic.

In this chapter, we explain and express mathematically the relationship between the perturbed refractive index of Eq. (2.1) and the perturbed reflectance of Eq. (2.2). In order to do so, two physical phenomena, i.e. *reflection* and *optical interference*, as well as their causes need to be introduced.

First, *reflection* occurs when an electromagnetic wave reaches an interface between two media with different complex refractive indices (see Fig. 2.1). The boundary conditions of Maxwell's wave equations indeed show that only a proportion $\tilde{t}$ of the electromagnetic wave is transmitted through the interface. The rest of it, i.e. a proportion $\tilde{r} = \tilde{t} - 1$, bounces back or *is reflected* in opposite direction [1].

In other words, for an incident electric field $\tilde{E}_i$, the transmitted electric field is $\tilde{E}_t = \tilde{t}\tilde{E}_i$ and the reflected electric field is $\tilde{E}_r = \tilde{r}\tilde{E}_i$, where $\tilde{t}$ and $\tilde{r}$ are respectively called the transmission and reflection coefficients. Mathematically, the reflection coefficient $\tilde{r}$ of a light beam normally incident upon an interface separating two media with different complex refractive indices $\tilde{n}_1$ and $\tilde{n}_2$ follows Fresnel's reflection formula [1], i.e.

$$\tilde{r} = \frac{\tilde{n}_1 - \tilde{n}_2}{\tilde{n}_1 + \tilde{n}_2}. \tag{2.3}$$

The electromagnetic wave is therefore transmitted with a transmission coefficient $\tilde{t}$ such that

$$\tilde{t} = 1 + \tilde{r} = \frac{2\tilde{n}_1}{\tilde{n}_1 + \tilde{n}_2}. \tag{2.4}$$

The reflectance of the sample is then given by the squared absolute value of the reflection coefficient, i.e.

$$R = |\tilde{r}|^2 . \tag{2.5}$$

Second, *optical interference* is the name given to the interaction between two (or more) coherent light beams of the same optical frequency and polarization meeting in a region of space [2]. In summary, the interference describes the peculiar way these waves add up so as to give a total amplitude with is *not* simply the sum of their amplitudes.

Mathematically, the electric field of a one-dimensional electromagnetic plane wave in a medium of refractive index $\tilde{n}$ can be described as follows [1]

$$\tilde{E} = |E| \exp(2i\pi\tilde{n}x/\lambda_E + i\theta_E) \exp(-i\omega_E t), \tag{2.6}$$

where $|E|$ is the amplitude of the electric field (its maximum value in time and space), θ_E is its phase, λ_E is its wavelength in vacuum and ω_E is its optical angular frequency. If two electromagnetic waves of the same amplitude and different phases $\tilde{E}_1 = |E| \exp(2i\pi\tilde{n}x/\lambda_E + i\theta_{E1}) \exp(-i\omega_E t)$ and $\tilde{E}_2 = |E| \exp(2i\pi\tilde{n}x/\lambda_E + i\theta_{E2}) \exp(-i\omega_E t)$ meet, their amplitudes add up *vectorially* (or *coherently*) such that

$$\tilde{E_1} + \tilde{E_2} = |E| \left[\exp(i\theta_{E1}) + \exp(i\theta_{E2})\right] \exp(2i\pi\tilde{n}x/\lambda_E - i\omega_E t). \tag{2.7}$$

Equation (2.7) shows that the resulting amplitude is not solely dependent on the amplitude of the two beams but that it also strongly depends on their phase difference. If the two waves have the same phase (i.e. $\theta_{E1} = \theta_{E2}$), the amplitude of their sum is $2|E|$, i.e. there is *constructive interference*. On the contrary if the phases of the two waves are in opposition (i.e. $\theta_{E1} = \theta_{E2} + \pi$), the sum is zero, giving rise to *destructive interference*. For other values of the phase difference, the sum will be included between 0 and $2|E|$. Similarly, in the more general case of waves with different amplitudes $|E_1|$ and $|E_2|$, destructive and constructive interferences result in total fields of respective amplitudes $|E_1 - E_2|$ and $|E_1 + E_2|$.

One common case of interference arises when a light beam is reflected on two or more parallel interfaces. The case of two interfaces is well known and widely studied under the name of thin-film interference [2] (Fig. 2.2). In that case, $\tilde{E}_1$ is the electric field reflected directly on the top surface (Interface 1) and $\tilde{E}_2$ is the electric field reflected on the bottom surface (Interface 2). Due to distance traveled by $\tilde{E}_2$ in between the two interfaces, the phase difference between the two reflected electric fields is proportional to the thickness of the film. The combination of reflection and interference therefore offers a very attractive sensitivity to the thickness of a thin film. This is what makes reflection techniques so appealing. This experiment is studied in further detail in Sect. 2.2.

Due to interference effects, the mathematical relationships between the components of $\tilde{n}(x, y, z, t)$ and $R(x, y, t)$ vary according to the depth- (i.e. the z-) dependence of the refractive index perturbation. In this chapter, we investigate four different cases of refractive index perturbations and work out these relationships in order of

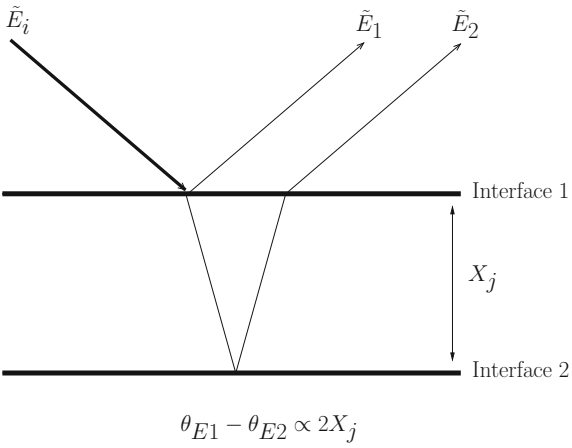

Fig. 2.2 Thin-film interference: the electric fields $\tilde{E}_1$ and $\tilde{E}_2$ respectively reflected on interface 1 and interface 2 present a phase difference $\theta_{E1} - \theta_{E2}$ due to the distance traveled by the light in between the two interfaces. As a consequence, the amplitude of the total reflected electric field varies with the thickness of the thin film

increasing complexity. First, uniform perturbations are studied in Sect. 2.1. In this case, the complex refractive index varies only at the top surface. Second, in Sect. 2.2, we consider the case of a box-like perturbation where the perturbed refractive index shows two abrupt variations, one at the top surface and one at a depth X_j, which we call the junction depth. Finally, we study the case of a double box-like perturbation (three abrupt variations) in Sect. 2.3 before deriving a formula for a perturbation with an arbitrary depth dependence in Sect. 2.4.

These analytical expressions are here derived in the case of TP, i.e. for a probe laser in the red to near infrared (NIR) range normally incident on the sample and for a system lying in air. As a consequence, the penetration depth of the probe laser $1/\alpha_{\text{probe}}$ is always much larger than the total depth of the perturbation of the complex refractive index (ultra-shallow perturbations) but much shorter than the thickness of the sample (semi-infinite samples). Further, we make the following three key assumptions so as to keep the expressions simple and analytical. First, the Si surface is supposed to be oxide-free, i.e. silicon is in direct contact with air. Second, we consider only laterally homogeneous refractive index perturbations, i.e. $\Delta\tilde{n}_j(x, y, z) = \Delta\tilde{n}_j(z)$ ($j = 0, 1, \ldots$). These first two assumptions are discussed into more detail at the end of this chapter respectively in Sects. 2.5.1 and 2.5.2. Finally, all the perturbation components of Eq. (2.1) are assumed much smaller than $\tilde{n}_0$. This linearizes the system (no harmonic mixing) and therefore greatly simplifies the obtained expressions. In other words, only a DC perturbation $\Delta\tilde{n}_0$ of the complex refractive index can induce a DC variation ΔR_0 in reflectance. Similarly, only the fundamental mode of the complex refractive index can generate ΔR_1. Besides, the relationships between the perturbation components of $\tilde{n}$ and R are the same independently from the considered component. We can therefore focus on a case of a single perturbation, relying on the linearity of the system for the cases of multiple perturbations. The j subscript ($j = 0, 1, \ldots$) is therefore omitted in the rest of this chapter.

For the sake of completeness, let us mention that two formulations are available to solve the considered problem. We propose to solve this problem in the *small*

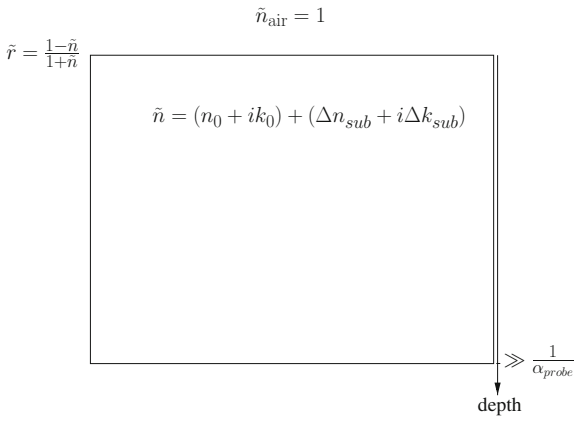

Fig. 2.3 A uniform perturbation $(\Delta n_{sub} + i\,\Delta k_{sub})$ of the refractive index $(n_0 + ik_0)$ of a semi-infinite sample

perturbation formalism in this chapter. The alternative formulation, i.e. the direct *differentiation*, was derived by Seraphin [3] and Aspnes [4, 5]. With some algebra, it can be shown that the two formulations are equivalent.

2.1 Uniform Perturbation of the Complex Refractive Index

In this Section, we consider a sample with a complex refractive index $(n_0 + ik_0)$ modified by a uniform perturbation $(\Delta n_{sub} + i\,\Delta k_{sub})$ and would like to calculate how this perturbation impacts the sample reflectance. The studied situation is depicted in Fig. 2.3.

In the case of a perturbed complex refractive index, Fresnel's formula (2.3) becomes

$$\tilde{r} = \frac{1 - (n_0 + ik_0) - (\Delta n_{sub} + i\,\Delta k_{sub})}{1 + (n_0 + ik_0) + (\Delta n_{sub} + i\,\Delta k_{sub})}. \tag{2.8}$$

Linearizing formula (2.8) with respect to the perturbation, $\tilde{r}$ becomes

$$\begin{aligned}
\tilde{r} &\approx \underbrace{\frac{1 - (n_0 + ik_0)}{1 + (n_0 + ik_0)}}_{=\tilde{r}_0} \left[\left(1 - \frac{\Delta n_{sub} + i\,\Delta k_{sub}}{1 - n_0 - ik_0} \right) \left(1 - \frac{\Delta n_{sub} + i\,\Delta k_{sub}}{1 + n_0 + ik_0} \right) \right] \\
&\approx \tilde{r}_0 \left[1 - \frac{2}{(1 - n_0 - ik_0)(1 + n_0 + ik_0)} (\Delta n_{sub} + i\,\Delta k_{sub}) \right] \\
&= \tilde{r}_0 \left\{ 1 - \frac{2\left[(1 - n_0^2 + k_0^2)\Delta n_{sub} - 2n_0 k_0 \Delta k_{sub} \right]}{(1 - n_0^2 + k_0^2)^2 + 4n_0^2 k_0^2} \right. \\
&\qquad \left. - i \frac{2\left[(1 - n_0^2 + k_0^2)\Delta k_{sub} + 2n_0 k_0 \Delta n_{sub} \right]}{(1 - n_0^2 + k_0^2)^2 + 4n_0^2 k_0^2} \right\},
\end{aligned} \tag{2.9}$$

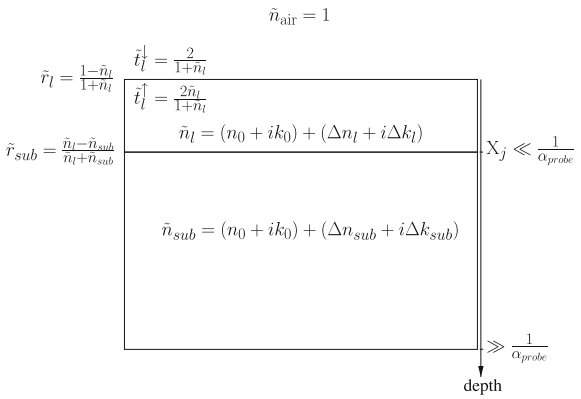

Fig. 2.4 A box-like perturbation of the refractive index profile shows two abrupt variations, respectively at the surface and at the interface. The interface is located at a depth X_j assumed to be much smaller than the penetration depth of the probe laser $(1/\alpha_{\mathrm{probe}})$

where $\tilde{r}_0$ is the reflection coefficient of the unperturbed sample. The perturbed reflectance $R = |\tilde{r}|^2$ is therefore

$$R = \underbrace{|\tilde{r}_0|^2}_{=R_0} \left\{ 1 - \frac{4}{(1 - n_0^2 + k_0^2)^2 + 4n_0^2 k_0^2} \left[(1 - n_0^2 + k_0^2)\Delta n_{sub} - 2n_0 k_0 \Delta k_{sub} \right] \right\}. \tag{2.10}$$

Before concluding this Section, it is interesting to note that $\partial R/\partial \Delta k_{sub}$ is proportional to k_0, which is very small in silicon in the red and NIR range [6]. In other words, a uniform Δk_{sub} hardly perturbs the reflectance of silicon in the red and NIR range. Further neglecting all the k_0 terms of Eq. (2.10), the variation ΔR in reflectance for a homogeneous perturbation simply reads

$$\Delta R|_{\mathrm{homogeneous}} = \frac{4R_0}{n_0^2 - 1} \Delta n_{sub}. \tag{2.11}$$

This formula will prove very helpful for calculating the perturbation of the reflectance on a homogeneously doped sample, whether it is due to homogeneous doping, optically injected carriers or heat (Sect. 6.1).

2.2 Box-Like Perturbation of the Complex Refractive Index

We consider here the problem of a perturbation of the refractive index which only shows two abrupt transitions, one at the top surface and one at a depth X_j, called the junction depth. The perturbation of the refractive index has a value $(\Delta n_l + i\,\Delta k_l)$ in the box and a value $(\Delta n_{sub} + i\,\Delta k_{sub})$ below the layer. The unperturbed refractive index of the sample is uniform and equal to $(n_0 + ik_0)$. This situation is described

in Fig. 2.4. We recognize here the thin-film interference introduced earlier in the introduction of the present chapter.

If we assume that the magnitude of the perturbation of refractive index is too small to cause multireflections in the box [2], the pertubation of the reflection coefficient is solely due to the *coherent* sum of the two reflections occurring respectively at the surface and at the interface. Further, neglecting the impact of the refractive index perturbation on the phase of the transmitted electric field, the reflection coefficient is

$$\tilde{r} = \tilde{r}_1 + \tilde{r}_{sub}\tilde{t}^{\uparrow}\tilde{t}^{\downarrow}\exp(4i\pi n_0 X_j/\lambda_{\text{probe}}), \tag{2.12}$$

where $\tilde{r}_1$ and $\tilde{r}_{sub}$ are the reflection coefficients respectively at the surface and the interface, $\tilde{t}_l^{\downarrow}$ and $\tilde{t}_l^{\uparrow}$ are the transmission coefficients through the surface respectively for incoming and outgoing light.

In analogy to formula (2.9), we have for $\tilde{r}_l$

$$\begin{aligned}\tilde{r}_l = \tilde{r}_0\Bigg\{1 &- \frac{2\left[(1-n_0^2+k_0^2)\Delta n_l - 2n_0k_0\Delta k_l\right]}{(1-n_0^2+k_0^2)^2+4n_0^2k_0^2} \\ &- i\frac{2\left[(1-n_0^2+k_0^2)\Delta k_l + 2n_0k_0\Delta n_l\right]}{(1-n_0^2+k_0^2)^2+4n_0^2k_0^2}\Bigg\}.\end{aligned} \tag{2.13}$$

As for $\tilde{r}_{sub}$, neglecting all second-order perturbation terms, one obtains

$$\begin{aligned}\tilde{r}_{sub} &= \frac{(\Delta n_l + i\Delta k_l) - (\Delta n_{sub} + i\Delta k_{sub})}{2(n_0+ik_0)+(\Delta n_l + i\Delta k_l)+(\Delta n_{sub}+i\Delta k_{sub})} \\ &\approx \frac{(\Delta n_l - \Delta n_{sub}) + i(\Delta k_l - \Delta k_{sub})}{2(n_0+ik_0)}.\end{aligned} \tag{2.14}$$

It is apparent from the comparison of Eqs. (2.13) and (2.14) that the surface and interface reflections have very different magnitudes. While the surface reflection is composed of two terms, respectively of the zeroth and first orders, the interface reflection only shows a first-order contribution. This is due to the fact that, unlike the surface reflection, the interface reflection only exists because of the perturbation. Since we neglect all second-order terms, using formula (2.4), we can write

$$\begin{aligned}\tilde{r}_{sub}\tilde{t}^{\uparrow}\tilde{t}^{\downarrow} &= 2\tilde{r}_0\frac{(\Delta n_l - \Delta n_{sub}) + i(\Delta k_l - \Delta k_{sub})}{(1-n_0-ik_0)(1+n_0+ik_0)} \\ &= 2\tilde{r}_0\Bigg\{\frac{(1-n_0^2+k_0^2)(\Delta n_l - \Delta n_{sub}) - 2k_0n_0(\Delta k_l - \Delta k_{sub})}{(1-n_0^2+k_0^2)^2+4n_0^2k_0^2} \\ &\quad + i\frac{(1-n_0^2+k_0^2)(\Delta k_l - \Delta k_{sub}) + 2k_0n_0(\Delta n_l - \Delta n_{sub})}{(1-n_0^2+k_0^2)^2+4n_0^2k_0^2}\Bigg\}.\end{aligned} \tag{2.15}$$

Putting Eqs. (2.12), (2.13) and (2.15) together and neglecting all second-order terms, this gives for the reflectance

$$
\begin{aligned}
R &\approx |\tilde{r}_l|^2 + 2\Re(\tilde{r}_0^\star \tilde{r}_{sub} \tilde{t}^\uparrow \tilde{t}^\downarrow \exp(4i\pi n_0 X_j/\lambda_{\text{probe}})) \\
&= R_0 \Bigg\{ 1 - \frac{4}{(1-n_0^2+k_0^2)^2 + 4n_0^2 k_0^2} \\
&\quad \times \Bigg[(1-n_0^2+k_0^2)\Delta n_l - 2n_0 k_0 \Delta k_l \\
&\quad - \Big((1-n_0^2+k_0^2)(\Delta n_l - \Delta n_{sub}) - 2k_0 n_0 (\Delta k_l - \Delta k_{sub}) \Big) \\
&\quad \times \cos(4\pi n_0 X_j/\lambda_{\text{probe}}) \\
&\quad + \Big((1-n_0^2+k_0^2)(\Delta k_l - \Delta k_{sub}) + 2k_0 n_0 (\Delta n_l - \Delta n_{sub}) \Big) \\
&\quad \times \sin(4\pi n_0 X_j/\lambda_{\text{probe}}) \Bigg] \Bigg\},
\end{aligned}
\tag{2.16}
$$

where $\tilde{r}_0^\star$ is the complex conjugate of $\tilde{r}_0$. Assuming again that $k_0 \ll n_0$, the perturbation of the reflectance is

$$
\begin{aligned}
\Delta R|_{\text{box}} = \frac{4R_0}{n_0^2-1} \big[&\Delta n_l \\
&- \cos(4\pi n_0 X_j/\lambda_{\text{probe}})(\Delta n_l - \Delta n_{sub}) \\
&+ \sin(4\pi n_0 X_j/\lambda_{\text{probe}})(\Delta k_l - \Delta k_{sub}) \big].
\end{aligned}
\tag{2.17}
$$

This equation is of very high importance in this work. It indeed shows the interest of reflection techniques for the depth-determination of a refractive index perturbation. Though reflection techniques are surface techniques, they are able to probe the in-depth variations in refractive index with high sensitivity thanks to the interference between the reflections respectively occuring at the surface and at the interface of the box. This is the main reason why optical reflection techniques are usually very attractive for the non-destructive determination of e.g. layer thicknesses [2]. Besides, Eq. (2.17) proves to explain with great accuracy the perturbed reflectances experimentally observed on CVD box-like doping profiles (Chap. 6.2). It will therefore be frequently used for the assessment of our model.

Notice finally that, if X_j=0, formula (2.17) nicely reduces to formula (2.11).

2.3 Double Box-Like Perturbation of the Complex Refractive Index

We consider here the problem of a perturbation of the refractive index which has three abrupt transitions, one at the top surface, one at a depth X_{j1} and a last one at a depth X_{j2}. This situation is shown in Fig. 2.5. The perturbation of the refractive index has a value $(\Delta n_{l1} + i\,\Delta k_{l1})$ in the top box, a value $(\Delta n_{l2} + i\,\Delta k_{l2})$ in the second

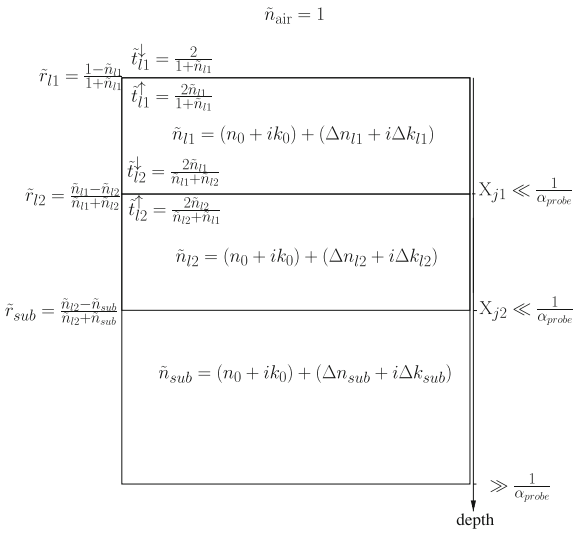

Fig. 2.5 A double box-like perturbation of the refractive index profile shows three abrupt variations, respectively at the surface, at a depth X_{j1} and at a depth X_{j2}

box and a value $(\Delta n_{sub} + i\,\Delta k_{sub})$ below the second box. The unperturbed refractive index of the sample is uniform and equal to $(n_0 + ik_0)$.

As can be expected, the perturbation of the reflection coefficient is here due to the coherent sum of the *three* reflections occurring at the surface and at the two interfaces. In other words, generalizing Eq. (2.12), the reflection coefficient can be written

$$\tilde{r} = \tilde{r}_{l1} + \tilde{r}_{l2}\tilde{t}_{l1}^{\uparrow}\tilde{t}_{l1}^{\downarrow}\exp(4i\pi n_0 X_{j1}/\lambda_{\text{probe}}) + \tilde{r}_{sub}\tilde{t}_{l1}^{\uparrow}\tilde{t}_{l1}^{\downarrow}\tilde{t}_{l2}^{\uparrow}\tilde{t}_{l2}^{\downarrow}\exp(4i\pi n_0 X_{j2}/\lambda_{\text{probe}}). \tag{2.18}$$

In analogy with Eq. (2.9) for $\tilde{r}_{l1}$ and Eq. (2.14) for $\tilde{r}_{l2}$ and $\tilde{r}_{sub}$, the reflection coefficients on each interface are respectively

$$\tilde{r}_{l1} = \tilde{r}_0\left\{1 - \frac{2\left[(1-n_0^2+k_0^2)\Delta n_{l1} - 2n_0k_0\Delta k_{l1}\right]}{(1-n_0^2+k_0^2)^2 + 4n_0^2k_0^2} - i\frac{2\left[(1-n_0^2+k_0^2)\Delta k_{l1} + 2n_0k_0\Delta n_{l1}\right]}{(1-n_0^2+k_0^2)^2 + 4n_0^2k_0^2}\right\} \tag{2.19}$$

$$\tilde{r}_{l2} = \frac{(\Delta n_{l1} - \Delta n_{l2}) + i(\Delta k_{l1} - \Delta k_{l2})}{2(n_0 + ik_0)} \tag{2.20}$$

$$\tilde{r}_{sub} = \frac{(\Delta n_{l2} - \Delta n_{sub}) + i(\Delta k_{l2} - \Delta k_{sub})}{2(n_0 + ik_0)}. \tag{2.21}$$

Similarly to Eq. (2.15), we have

$$\tilde{r}_{l2}\tilde{t}_{l1}^{\uparrow}\tilde{t}_{l1}^{\downarrow} = 2\tilde{r}_0\left\{\frac{(1-n_0^2+k_0^2)(\Delta n_{l1}-\Delta n_{l2})-2k_0n_0(\Delta k_{l1}-\Delta k_{l2})}{(1-n_0^2+k_0^2)^2+4n_0^2k_0^2}\right.$$
$$\left.+\,i\,\frac{(1-n_0^2+k_0^2)(\Delta k_{l1}-\Delta k_{l2})+2k_0n_0(\Delta n_{l1}-\Delta n_{l2})}{(1-n_0^2+k_0^2)^2+4n_0^2k_0^2}\right\} \quad (2.22)$$

$$\tilde{r}_{sub}\tilde{t}_{l1}^{\uparrow}\tilde{t}_{l1}^{\downarrow}t_{l2}^{\uparrow}\tilde{t}_{l2}^{\downarrow} = 2\tilde{r}_0\left\{\frac{(1-n_0^2+k_0^2)(\Delta n_{l2}-\Delta n_{sub})-2k_0n_0(\Delta k_{l2}-\Delta k_{sub})}{(1-n_0^2+k_0^2)^2+4n_0^2k_0^2}\right.$$
$$\left.+\,i\,\frac{(1-n_0^2+k_0^2)(\Delta k_{l2}-\Delta k_{sub})+2k_0n_0(\Delta n_{l2}-\Delta n_{sub})}{(1-n_0^2+k_0^2)^2+4n_0^2k_0^2}\right\}. \quad (2.23)$$

Plugging Eqs. (2.19), (2.22) and (2.23) into Eq. (2.18) and neglecting all second-order terms in refractive index variations, we have

$$\begin{aligned}
R &= |\tilde{r}_{l1}|^2 \\
&\quad + 2\Re(\tilde{r}_0^{\star}\tilde{r}_{l2}\tilde{t}_{l1}^{\uparrow}\tilde{t}_{l1}^{\downarrow}\exp(4i\pi n_0 X_{j1}/\lambda_{\text{probe}})) \\
&\quad + 2\Re(\tilde{r}_0^{\star}\tilde{r}_{sub}\tilde{t}_{l1}^{\uparrow}\tilde{t}_{l1}^{\downarrow}\tilde{t}_{l2}^{\uparrow}\tilde{t}_{l2}^{\downarrow}\exp(4i\pi n_0 X_{j2}/\lambda_{\text{probe}})) \\
&= R_0\left\{1-\frac{4}{(1-n_0^2+k_0^2)^2+4n_0^2k_0^2}\right. \\
&\quad \times\left[(1-n_0^2+k_0^2)\Delta n_{l1}-2n_0k_0\Delta k_{l1}\right. \\
&\quad -\left((1-n_0^2+k_0^2)(\Delta n_{l1}-\Delta n_{l2})-2k_0n_0(\Delta k_{l1}-\Delta k_{l2})\right) \\
&\quad \times\cos(4\pi n_0 X_{j1}/\lambda_{\text{probe}}) \\
&\quad +\left((1-n_0^2+k_0^2)(\Delta k_{l1}-\Delta k_{l2})+2k_0n_0(\Delta n_{l1}-\Delta n_{l2})\right) \\
&\quad \times\sin(4\pi n_0 X_{j1}/\lambda_{\text{probe}}) \\
&\quad -\left((1-n_0^2+k_0^2)(\Delta n_{l2}-\Delta n_{sub})-2k_0n_0(\Delta k_{l2}-\Delta k_{sub})\right) \\
&\quad \times\cos(4\pi n_0 X_{j2}/\lambda_{\text{probe}}) \\
&\quad +\left((1-n_0^2+k_0^2)(\Delta k_{l2}-\Delta k_{sub})+2k_0n_0(\Delta n_{l2}-\Delta n_{sub})\right) \\
&\quad \left.\left.\times\sin(4\pi n_0 X_{j2}/\lambda_{\text{probe}})\right]\right\}. \quad (2.24)
\end{aligned}$$

Assuming again that $k_0 \ll n_0$, the perturbation of the reflectance is

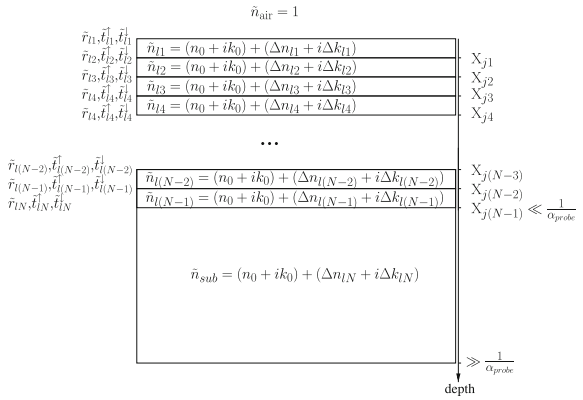

Fig. 2.6 A staircase perturbation of the refractive index profile with N abrupt transitions

$$\begin{aligned}\Delta R|_{\text{double-box}} = \frac{4R_0}{(n_0^2-1)}\Big[&\Delta n_{l1}\\ &-\cos(4\pi n_0 X_{j1}/\lambda_{\text{probe}})(\Delta n_{l1}-\Delta n_{l2})\\ &-\cos(4\pi n_0 X_{j2}/\lambda_{\text{probe}})(\Delta n_{l2}-\Delta n_{sub})\\ &+\sin(4\pi n_0 X_{j1}/\lambda_{\text{probe}})(\Delta k_{l1}-\Delta k_{l2})\\ &+\sin(4\pi n_0 X_{j2}/\lambda_{\text{probe}})(\Delta k_{l2}-\Delta k_{sub})\Big]. \end{aligned} \tag{2.25}$$

2.4 Arbitrary Perturbation of the Complex Refractive Index

Building the theory as we have, it is now fairly easy to derive a general formula for a staircase perturbation of the complex refractive index with N abrupt transitions such as presented in Fig. 2.6.

Generalizing Eqs. (2.12) and (2.18) for the case of an N-transition staircase gives

$$\begin{aligned}\tilde{r} = {}&\tilde{r}_{l1} + \tilde{r}_{l2}\tilde{t}^{\uparrow}_{l1}\tilde{t}^{\downarrow}_{l1}\exp(4i\pi n_0 X_{j1}/\lambda_{\text{probe}}) + \tilde{r}_{l3}\tilde{t}^{\uparrow}_{l1}\tilde{t}^{\downarrow}_{l1}\tilde{t}^{\uparrow}_{l2}\tilde{t}^{\downarrow}_{l2}\exp(4i\pi n_0 X_{j2}/\lambda_{\text{probe}})\\ &+\cdots\\ &+\tilde{r}_{l(N-1)}\tilde{t}^{\uparrow}_{l1}\tilde{t}^{\downarrow}_{l1}\tilde{t}^{\uparrow}_{l2}\tilde{t}^{\downarrow}_{l2}\ldots\tilde{t}^{\uparrow}_{l(N-2)}\tilde{t}^{\downarrow}_{l(N-2)}\exp(4i\pi n_0 X_{j(N-2)}/\lambda_{\text{probe}})\\ &+\tilde{r}_{lN}\tilde{t}^{\uparrow}_{l1}\tilde{t}^{\downarrow}_{l1}\tilde{t}^{\uparrow}_{l2}\tilde{t}^{\downarrow}_{l2}\ldots\tilde{t}^{\uparrow}_{l(N-1)}\tilde{t}^{\downarrow}_{l(N-1)}\exp(4i\pi n_0 X_{j(N-1)}/\lambda_{\text{probe}}). \end{aligned} \tag{2.26}$$

The expression for the surface reflection $\tilde{r}_{l1}$ is given by Eq. (2.19). As for the other reflections $\tilde{r}_{l\eta}$ ($\eta = 2, 3, \ldots, N$), a generalization of Eq. (2.20) gives

$$\tilde{r}_{l\eta} = \frac{(\Delta n_{l(\eta-1)} - \Delta n_{l\eta}) + i(\Delta k_{l(\eta-1)} - \Delta k_{l\eta})}{2(n_0 + ik_0)}. \tag{2.27}$$

Generalizing Eq. (2.22), we therefore have

$$\begin{aligned}
&\tilde{r}_{l\eta}\tilde{t}^{\uparrow}_{l1}\tilde{t}^{\downarrow}_{l1}\ldots\tilde{t}^{\uparrow}_{l(\eta-1)}\tilde{t}^{\downarrow}_{l(\eta-1)}\\
&\quad= 2\tilde{r}_0\left\{\frac{(1-n_0^2+k_0^2)(\Delta n_{l(\eta-1)}-\Delta n_{l\eta})-2k_0n_0(\Delta k_{l(\eta-1)}-\Delta k_{l\eta})}{(1-n_0^2+k_0^2)^2+4n_0^2k_0^2}\right.\\
&\qquad\left.+\,i\frac{(1-n_0^2+k_0^2)(\Delta k_{l(\eta-1)}-\Delta k_{l\eta})+2k_0n_0(\Delta n_{l(\eta-1)}-\Delta n_{l\eta})}{(1-n_0^2+k_0^2)^2+4n_0^2k_0^2}\right\}. \qquad (2.28)
\end{aligned}$$

which gives the reflectance when plugged into the following generalization of Eq. (2.24)

$$\begin{aligned}
&R=|\tilde{r}_{l1}|^2\\
&\quad+2\Re\left(\tilde{r}_0^{\star}\sum_{\eta=2}^{N}\tilde{r}_{l\eta}t^{\uparrow}_{l1}\tilde{t}^{\downarrow}_{l1}\ldots t^{\uparrow}_{l(\eta-1)}\tilde{t}^{\downarrow}_{l(\eta-1)}\exp(4i\pi n_0X_{j(\eta-1)}/\lambda_{\text{probe}})\right). \qquad (2.29)
\end{aligned}$$

If the thickness of the layers becomes infinitesimal, i.e. the perturbation of the refractive index varies continuously with depth, Eq. (2.27) becomes

$$\begin{aligned}
\tilde{r}_{l\eta}&=\frac{d(\Delta n+i\Delta k)}{2(n_0+ik_0)}\\
&=\frac{1}{2(n_0+ik_0)}\frac{\partial(\Delta n+i\Delta k)}{\partial z}dz, \qquad (2.30)
\end{aligned}$$

and the sum appearing in Eq. (2.29) must be turned into an integral to give

$$\begin{aligned}
R&=|\tilde{r}_{l1}|^2+2\Re\left(\tilde{r}_0^{\star}\frac{2\tilde{r}_0}{(1-n_0-ik_0)(1+n_0+ik_0)}\right.\\
&\qquad\left.\times\int_{0+}^{+\infty}\frac{\partial(\Delta n+i\Delta k)}{\partial z}\exp(4i\pi n_0z/\lambda_{\text{probe}})dz\right)\\
&=R_0\left\{1-\frac{4}{(1-n_0^2+k_0^2)^2+4n_0^2k_0^2}\times\left[(1-n_0^2+k_0^2)\Delta n(z=0)-2n_0k_0\Delta k(z=0)\right.\right.\\
&\quad+(1+n_0^2+k_0^2)\left(\int_{0+}^{+\infty}\frac{\partial\Delta n(z)}{\partial z}\cos(4\pi n_0z/\lambda_{\text{probe}})dz-\frac{\partial\Delta k(z)}{\partial z}\sin(4\pi n_0z/\lambda_{\text{probe}})dz\right)\\
&\quad\left.\left.+2k_0n_0\left(\int_{0+}^{+\infty}\frac{\partial\Delta k(z)}{\partial z}\cos(4\pi n_0z/\lambda_{\text{probe}})dz+\frac{\partial\Delta n(z)}{\partial z}\sin(4\pi n_0z/\lambda_{\text{probe}})dz\right)\right]\right\}. \qquad (2.31)
\end{aligned}$$

For Si in the red and NIR range, Eq. (2.31) becomes

$$\Delta R|_{\text{Profile}} = \frac{4R_0}{(n_0^2-1)}\left[\Delta n(z=0) + \int_{0+}^{+\infty}\left(\frac{\partial \Delta n(z)}{\partial z}\cos(4\pi n_0 z/\lambda_{\text{probe}}) - \frac{\partial \Delta k(z)}{\partial z}\sin(4\pi n_0 z/\lambda_{\text{probe}})\right)dz\right]. \tag{2.32}$$

It can be easily checked that in the case of a box-like perturbation of the refractive index, formula (2.32) reduces to (2.17).

2.5 Second-Order Effects

As mentioned in the Introduction, the reflection formulas derived in this chapter assume the absence of any oxide layer at the interface between air and the silicon sample. Similarly, the derived formulas only consider laterally homogeneous perturbations of the refractive index. These two assumptions are respectively looked at in Sects. 2.5.1 and 2.5.2 below.

2.5.1 Impact of the Presence of a Native Oxide

An oxide always exists at the interface between air and silicon. Hence, its impact should be evaluated. For this purpose, we propose to consider the case of a box-like perturbation of the refractive index, as studied in Sect. 2.2. On top of the structure of Fig. 2.4, we add an oxide layer of thickness t_{oxide} and of refractive index[1] $n_{\text{oxide}} = 1.45$ [7], such as represented in Fig. 2.7.

This effect should be studied as a function of t_{oxide} but, since the native oxides present on our samples have measured thicknesses between 0 and 2 nm, we take the worst-case scenario, i.e $t_{\text{oxide}} = 2\,\text{nm}$. We further assume that the refractive index perturbation does not propagate into the oxide. Figure 2.8 shows that, for a real refractive index perturbation with $\Delta n_{sub} = -10^{-4}$ (typical value encountered in the present work) and $\lambda_{\text{probe}} = 670\,\text{nm}$, the normalized variation $|(\Delta R_{\text{Box}}^{\text{Oxide}} - \Delta R_{\text{Box}})/\Delta R_{\text{Box}}(X_j = 0)|$ in reflectance perturbation is no more than 1.2 % whether $\Delta n_l = 0$ or -0.5×10^{-4}.

[1] Given the large refractive index contrast both at the air-oxide interface and at the oxide-silicon interface, multireflection formula [2] must be considered in the oxide layer (large reflection coefficients at both interfaces)

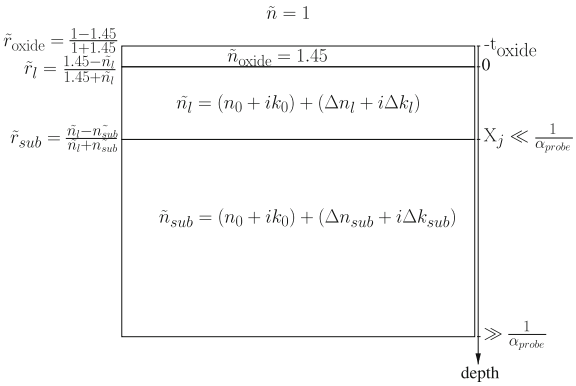

Fig. 2.7 Oxide layer of thickness t_{oxide} on top of a box-like perturbation of the refractive index profile

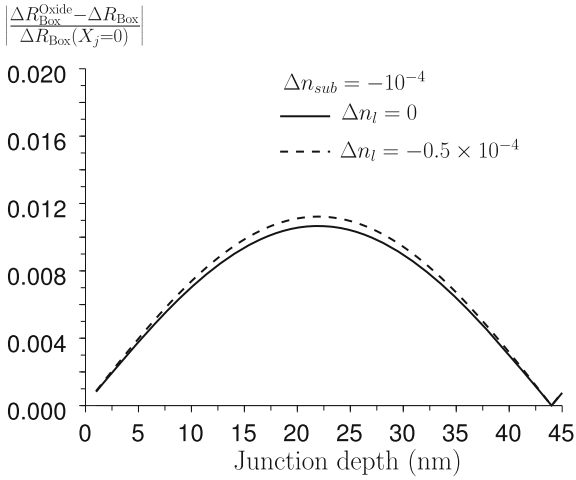

Fig. 2.8 Normalized variation $|(\Delta R_{\text{Box}}^{\text{Oxide}} - \Delta R_{\text{Box}})/\Delta R_{\text{Box}}(X_j = 0)|$ in reflectance perturbation due to the presence of a 2-nm thick oxide layer as a function of the junction depth of the box-like perturbation of the refractive index. The considered real values of the refractive index perturbation are indicated. The presence of the 2-nm thick native only has a negligible impact on the reflectance perturbation

For completeness, note that Fig. 2.8 does not show the behavior of the relative error $(\Delta R_{\text{Box}}^{\text{Oxide}} - \Delta R_{\text{Box}})/\Delta R_{\text{Box}}$. This error indeed diverges at $X_j \approx \lambda_{\text{probe}}/(8n_0) \approx 22\,\text{nm}$, due to the vanishing amplitude of ΔR_{Box}. As Fig. 2.8 shows, the absolute error remains small even at $X_j \approx 22\,\text{nm}$.

In summary, this effect can be neglected. It is, however, important to keep in mind that the variation grows with increasing oxide thickness.

2.5.2 Impact of a Lateral Variation in Refractive Index Perturbation

Thus far in this chapter, only laterally homogeneous perturbations of the refractive index have been considered. If $\Delta\tilde{n}(x, y, z)$ also varies with x and y, this effect will obviously be mirrored on the local reflectance perturbation $\Delta R(x, y)$. Typically, in this work, reflectance perturbations radially decay as damped waves (see Chap. 6), i.e.

$$\Delta R(r) = \Delta R(r = 0) \exp(-r/L_d^R) \cos(2\pi r/\Lambda^R), \tag{2.33}$$

where $r = \sqrt{x^2 + y^2}$ is defined as the radial distance to the maximum of the perturbation, L_d^R is the decay length and Λ^R is the wavelength of the reflectance perturbation. Figure 2.9a shows three examples of (normalized) reflectance perturbations behaving like damped waves with decay length $L_d^R = 2\,\mu\text{m}$ and respective wavelengths $\Lambda^R = 100, 10$ and $1\,\mu\text{m}$. As shown in Chap. 6, this is a relevant range for our experiments.

The probe laser irradiance distribution $\Pi_{\text{probe}}(r)$ being

$$\Pi_{\text{probe}}(r) = \mathcal{P}^0_{\text{probe}} \exp\left(-\frac{r^2}{\mathcal{R}^2_{\text{probe}}}\right), \tag{2.34}$$

where $\mathcal{P}^0_{\text{probe}}$ is the peak irradiance of the probe laser and $\mathcal{R}_{\text{probe}}$ is its radius, the measured reflectance perturbation $\Delta R_{\text{integrated}}$ will be a convolution of the local reflectance perturbation $\Delta R(r)$ with the probe laser irradiance distribution, i.e.

$$\begin{aligned}\Delta R_{\text{integrated}} &= \frac{2}{\mathcal{R}^2_{\text{laser}}} \int_0^\infty r dr \Delta R(r) \exp\left(-\frac{r^2}{\mathcal{R}^2_{\text{laser}}}\right) \\ &= \frac{2}{\mathcal{R}^2_{\text{laser}}} \int_0^\infty r dr \Delta R(r = 0) \exp(-r/L_d^R) \cos(2\pi r/\Lambda^R) \exp\left(-\frac{r^2}{\mathcal{R}^2_{\text{laser}}}\right),\end{aligned} \tag{2.35}$$

Note that we willingly restrict the present study to the case of corresponding positions of the maximum of the reflectance perturbation and of the probe irradiance.

Figure 2.9b shows the ratio of $\Delta R_{\text{integrated}}$, i.e. the reflectance perturbation as measured by the probe laser, divided by the local reflectance perturbation at $r = 0$, i.e. $\Delta R(r = 0)$. Obviously, when the decay length and wavelength are both long, $\Delta R_{\text{integrated}}$ is very close to $\Delta R(r = 0)$. This is the situation encountered in a vast majority ($> 95\,\%$) of our measurements, as highlighted by the dotted box in Fig. 2.9b. On the contrary, if the decay length and/or the wavelength become commensurate with $\mathcal{R}_{\text{probe}}$, strong deviations are observed, which can even lead to $\Delta R_{\text{integrated}}$

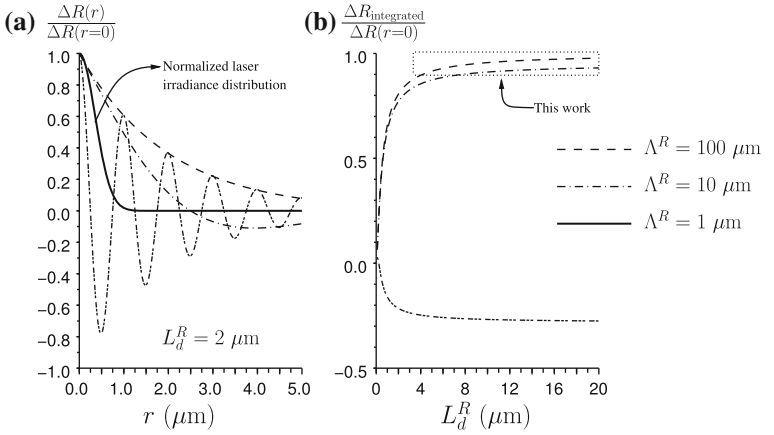

Fig. 2.9 **a** Examples of normalized reflectance perturbations behaving like damped waves (Eq. (2.33)) with decay length $L_d^R = 2\,\mu\mathrm{m}$ and $\Lambda^R = 100\,\mu\mathrm{m}$ (*dashed line*), $\Lambda^R = 10\,\mu\mathrm{m}$ (*interrupted line*) and $\Lambda^R = 1\,\mu\mathrm{m}$ (*triple-interrupted line*). The thick *black line* is the normalized irradiance distribution (Eq. (2.34) with $\mathcal{R}_{\mathrm{probe}} = 0.5\,\mu\mathrm{m}$). **b** Variation in the ratio of the integrated reflectance perturbation (Eq. (2.35)) divided by the signal at $r = 0$ as a function of the decay length of the reflectance perturbation. The dotted box shows the typical situations found in this work, where the impact of the lateral integration is minor

and $\Delta R(r = 0)$ being of opposite sign ($\Lambda^R = 1\,\mu\mathrm{m}$). In these cases, the lateral integration cannot be ignored.

In this study, we try to work with analytical expressions as much as possible. The lateral integration of Eq. (2.35) will therefore be omitted in our model. If required, however, our calculations can take it into account. Only minor impact of this effect has been observed for the specific case of the structures measured in this work. This justifies the omission in the rest of this dissertation.

2.6 Summary

In this chapter, we have investigated the mathematical relationship between a refractive index perturbation and the subsequent perturbation of the sample reflectance, as can be measured by a probe laser in the red and NIR range. We have shown that, due to interference effects, the relationships vary greatly according to the depth-dependence of the refractive index perturbation. Of particular importance in this work, we have derived analytical expressions in the cases of a homogeneous refractive index perturbation

$$\Delta R|_{\mathrm{homogeneous}} = \frac{4R_0}{n_0^2 - 1}\Delta n_{sub}, \tag{2.36}$$

in the case of a box-like refractive index perturbation

$$\begin{aligned}\Delta R|_{\text{box}} = \frac{4R_0}{n_0^2 - 1}\big[&\Delta n_l \\ &- \cos(4\pi n_0 X_j/\lambda_{\text{probe}})(\Delta n_l - \Delta n_{sub}) \\ &+ \sin(4\pi n_0 X_j/\lambda_{\text{probe}})(\Delta k_l - \Delta k_{sub})\big],\end{aligned} \tag{2.37}$$

and in the case of an arbitrary profile of refractive index perturbation

$$\begin{aligned}\Delta R|_{\text{Profile}} = \frac{4R_0}{(n_0^2 - 1)}\Bigg[&\Delta n(z=0) \\ &+ \int_{0+}^{+\infty}\left(\frac{\partial \Delta n(z)}{\partial z}\cos(4\pi n_0 z/\lambda_{\text{probe}}) - \frac{\partial \Delta k(z)}{\partial z}\sin(4\pi n_0 z/\lambda_{\text{probe}})\right)dz\Bigg],\end{aligned} \tag{2.38}$$

all the symbols being as defined in this chapter.

Further, we have shown that these expressions are valid even in the presence of a thin native oxide and in the case of laterally varying refractive index perturbations provided the lateral variations are not too abrupt.

References

1. M. Born, E. Wolf, *Principles of Optics* (Pergamon, Oxford, 1970)
2. H. Fujiwara, *Spectroscopic Ellipsometry: Principles and Applications* (Wiley, Chichester, 2007)
3. B.O. Seraphin, N. Bottka, Band-structure analysis from electro-reflectance studies. Phys. Rev. **145**(2), 628–636 (1966). doi:10.1103/PhysRev.145.628
4. D.E. Aspnes, in *Handbook on Semiconductors: Modulation Spectroscopy*, ed. by T.S. Moss (North Holland, New York, 1980)
5. D.E. Aspnes, A. Frova, Influence of spatially dependent perturbations on modulated reflectance and absorption of solids (reprinted in solid-state commun, vol 7, pg 155–159, 1969). Solid State Commun. **88**(11–12), 1061–1065 (1993)
6. T. Yasuda, D.E. Aspnes, Optical-standard surfaces of single-crystal silicon for calibrating ellipsometers and reflectometers. Appl. Opt. **33**(31), 7435–7438 (1994)
7. R. Hull (ed.), *Properties of Crystalline Silicon*, Emis Datareviews Series (INSPEC, London, 1999a)